

RVC OPEN ACCESS REPOSITORY – COPYRIGHT NOTICE

This is a pre-copyedited, author-produced version of an article accepted for publication in *Endocrinology* following peer review.

The version of record is available online at <https://doi.org/10.1210/en.2014-1572>.

The full details of the published version of the article are as follows:

TITLE: Excessive growth hormone expression in male GH transgenic mice adversely alters bone architecture and mechanical strength

AUTHORS: S. V. Lim M. Marenzana M. Hopkinson E. O. List J. J. Kopchick M. Pereira B. Javaheri J. P. Roux P. Chavassieux M. Korbonits C. Chenu

JOURNAL TITLE: *Endocrinology*

PUBLICATION DATE: April 2015

PUBLISHER: Oxford University Press

DOI: 10.1210/en.2014-1572

1 **Excessive Growth Hormone Expression in Male GH Transgenic Mice Adversely Alters Bone**
2 **Architecture and Mechanical Strength**

3

4 S. V. Lim, M. Marenzana, M. Hopkinson, E. O. List, J. J. Kopchick, M. Pereira, B. Javaheri, J. P. Roux, P.
5 Chavassieux, M. Korbonits, and C. Chenu

6

7 Department of Comparative and Biomedical Sciences (S.V.L., M.H., M.P., B.J., C.C.), Royal Veterinary
8 College, London NW1 0TU, United Kingdom;

9 Imperial College (M.M.), London SW7 2AZ, United Kingdom;

10 Edison Biotechnology Institute (E.O.L., J.J.K.), Ohio University, Ohio 45701;

11 INSERM Unité Mixte de Recherche 1033 and Université de Lyon (J.P.R., P.C.), 69372 Lyon Cedex 08,
12 France;

13 Department of Endocrinology (M.K.), Barts and the London School of Medicine, Queen Mary
14 University of London, London EC1A 6BQ, United Kingdom

15 Corresponding author: cchenu@rvc.ac.uk

16 **Abstract**

17 Patients with acromegaly have a higher prevalence of vertebral fractures despite normal bone
18 mineral density (BMD), suggesting that GH overexpression has adverse effects on skeletal
19 architecture and strength. We used giant bovine GH (bGH) transgenic mice to analyze the effects of
20 high serum GH levels on BMD, architecture, and mechanical strength. Five-month-old hemizygous
21 male bGH mice were compared with age- and sex-matched nontransgenic littermates controls (NT;
22 n=16/group). Bone architecture and BMD were analyzed in tibia and lumbar vertebrae using
23 microcomputed tomography. Femora were tested to failure using three-point bending and bone
24 cellular activity determined by bone histomorphometry. bGH transgenic mice displayed significant
25 increases in body weight and bone lengths. bGH tibia showed decreases in trabecular bone volume
26 fraction, thickness, and number compared with NT ones, whereas trabecular pattern factor and
27 structure model index were significantly increased, indicating deterioration in bone structure.
28 Although cortical tissue perimeter was increased in transgenic mice, cortical thickness was reduced.
29 bGH mice showed similar trabecular BMD but reduced trabecular thickness in lumbar vertebra
30 relative to controls. Cortical BMD and thickness were significantly reduced in bGH lumbar vertebra.
31 Mechanical testing of femora confirmed that bGH femora have decreased intrinsic mechanical
32 properties compared with NT ones. Bone turnover is increased in favor of bone resorption in bGH
33 tibia and vertebra compared with controls, and serum PTH levels is also enhanced in bGH mice.
34 These data collectively suggest that high serum GH levels negatively affect bone architecture and
35 quality at multiple skeletal sites.

36 Introduction

37 GH is a peptide hormone secreted by the anterior pituitary gland, which has catabolic and
38 anabolic actions on many organ systems. In the skeleton, it facilitates linear bone growth by causing
39 chondrocyte proliferation at the epiphyseal cartilage in the growth plate region (1,–3). GH also has
40 numerous metabolic functions regulating carbohydrate and lipid metabolism (4). It induces
41 intracellular signals through the GH receptor (GHR), a predimerized cytokine receptor signaling
42 through the Janus kinase (JAK)-signal transducer and activator of transcription pathway (STAT) (5).
43 Many of the growth-promoting actions of GH are mediated by IGF-1, which is synthesized in most
44 peripheral tissues, with liver synthesis contributing primarily to circulating IGF-1 levels (1). Both GH
45 and IGF-1 are anabolic hormones for the skeleton and are involved in the stimulation of bone
46 formation (1, 6). Although they have overlapping effects, GH and IGF-1 also have distinct effects on
47 skeletal development, bone growth, and fracture risk (7).

48 The importance of GH in the regulation of bone growth is best seen in patients with GH
49 deficiency (GHD) or GH excess (8, 9). Patients with GHD have a low bone turnover, whereas excess
50 GH, usually due to a GH-secreting pituitary tumor causing acromegaly, is associated with increased
51 bone turnover (9, 10). Although patients with acromegaly have characteristically enlarged bones and
52 excess cortical bone and osteophytes, clinical reports and experimental studies have shown
53 inconsistent data on bone mineral density (BMD) and, paradoxically, a number of studies suggested
54 increased fracture risk in these patients (11,–16). The clinical picture regarding bone is complicated
55 by the fact that patients with acromegaly often have hypogonadism due to excess prolactin
56 secretion and/or reduced gonadotropins due to tumor pressure effects. In active acromegaly, high
57 GH levels are associated with increased cortical BMD, whereas the effects on trabecular BMD are
58 more variable (17,–20). In addition, fracture risk in acromegaly was shown to be either associated
59 with BMD or independent of it, suggesting that BMD alone is not a sufficient indicator of fracture
60 risk (12,–14, 21). The effects of an excess GH on bone architecture and strength are still unclear.
61 Bone fracture risk is dependent on the overall bone strength, which itself depends on bone
62 structural and material properties, both of which are affected by bone turnover (22). Structural
63 properties of bone include its geometry and architecture (23), whereas its material properties
64 depend mainly on bone mineral and collagen contents that are affected by the rate of bone
65 remodeling (24).

66 Several transgenic animal models have been developed to study the effects of GH on bone.
67 Transgenic expression of bovine GH (bGH) or rat GH in mice is now commonly used to study GH
68 physiology, and GH is often fused with a transcriptional regulatory element such as the

69 metallothionein promoter/enhancer whose expression is constitutive (25,–27). Also,
70 supraphysiological levels of GH are usually found in these GH transgenic mice (25). Although several
71 studies have shown changes in bone growth, turnover and BMD in transgenic mice overexpressing
72 GH (26, 28,–30), there has been no extensive characterization of the three-dimensional bone
73 microarchitecture in cortical and trabecular compartments in relation with bone strength in those
74 mice.

75 The aim of this study was to examine whether the observed higher prevalence of vertebral
76 fractures in acromegaly patients (11,–15) could be explained by a compromised bone architecture
77 and strength. We used giant bGH transgenic mice to examine the effects of high serum GH and IGF-1
78 levels on BMD, on vertebra and tibia trabecular, and cortical bone architecture as well as on
79 mechanical strength in comparison with nontransgenic littermates control mice of the same age and
80 sex. Moreover, this work served to ascertain the potential of this transgenic mouse model for
81 further studies of the skeletal changes associated with acromegaly.

82 **Materials and methods**

83 *Animals*

84 bGH transgenic mice and nontransgenic littermates controls (NT) were generated as
85 described by Berryman et al (27). Briefly, bGH transgenic mice were generated using a
86 metallothionein transcriptional regulatory element linked to the first exon and intron of the bGH
87 cDNA. C57BL/6J embryos were injected with this construct, and the mice were maintained in the
88 genetic background. In our study, we used 5-month-old male mice and a total of 16 mice for each
89 genotype (NT and bGH) were analyzed. Blood was collected immediately after killing for hormone
90 measurements. The left tibiae and femora as well as lumbar vertebrae of 16 mice/group were
91 dissected, fixed in 10% neural-buffered formalin for 24–72 hours, and stored in 70% ethanol at 4°C
92 for microcomputed tomography (micro-CT) analysis of BMD and bone architecture. Right femora
93 were dissected and stored at –20°C for mechanical testing. To label bone-forming surfaces in
94 trabecular bone, mice (nine per group) were injected ip with calcein (Sigma-Aldrich) on day 8 and
95 alizarin red complexone (Sigma-Aldrich) on day 3, prior to euthanasia. Right tibiae and L4 vertebrae
96 were collected from these mice for bone histomorphometry analysis.

97 *Micro-CT analysis of tibiae and vertebrae*

98 Tibiae were scanned using high resolution (5 µm pixel size) micro-CT (Skyscan 1172) at x-ray
99 energy settings of 50 kV and 200 µA, using a 0.5 mm aluminum filter. Skyscan software was used for
100 computed tomography reconstructions (NRecon version 1.6.4.1) and bone histomorphometric

101 analyses in two and three dimensions (CT-Analyzer, version 1.13.5.1+) (31). The trabecular bone
102 analysis in tibiae was made in the proximal metaphysis. A reference point was chosen that
103 corresponds to the appearance of secondary spongiosa, and 50 tomograms below this reference
104 point were left unanalyzed before the analysis was made on 250 tomograms. The cortical bone was
105 excluded by operator-drawn regions of interest, and three-dimensional algorithms were used to
106 determine the relevant parameters including bone volume fraction [expressed as percentage of
107 bone volume (BV) over tissue volume (TV), trabecular thickness (Tb.Th), trabecular number (Tb.N),
108 trabecular separation (Tb.Sp), structure model index (SMI), trabecular bone pattern factor (Tb.Pf),
109 and the degree of anisotropy (DA)]. Analysis of cortical bone was performed along a 0.49-mm-long
110 segment (or 100 tomograms) at 37% and 50% of the full length of the tibia calculated from its
111 proximal end. For analysis of the cortical bone compartment, two-dimensional computation was
112 used, and parameters were determined for each of the 100 tomograms and then averaged.
113 Parameters included the following: total cross-sectional area (Tt.Ar), cortical bone area (Ct.Ar),
114 cortical bone perimeter (Ct.Pm), cross-sectional thickness (Ct.Th), and medullary area (Ma.Ar).
115 Cortical and trabecular bone architecture was also evaluated in L4 and L5 vertebrae using the same
116 settings as for tibiae. The region of interest included the whole body of vertebrae.

117 *BMD measurement in vertebrae*

118 BMD analysis in lumbar vertebrae (L4 and L5) was performed with Skyscan software (CT-
119 Analyzer, version 1.13.5.1+). BMD is defined as the volumetric density of calcium hydroxyapatite in
120 grams per cubic centimeter. Two Skyscan-supplied bone phantoms with known BMD values of 0.25
121 and 0.75 g/cm³ calcium hydroxyapatite were scanned and reconstructed with the same methods
122 and parameters as the vertebrae.

123 *Mechanical testing of femora*

124 Femora were excised immediately after the animals were killed, individually stored in saline
125 soaked gauze, and frozen at -20°C. Immediately before testing, they were thawed and immersed in
126 saline solution during the whole analysis. Three-point bending test of femora from NT and bGH mice
127 was performed as previously described (32). This test allows the calculation of a number of bone
128 mechanical properties, including resistance to bending under load (stiffness), the maximum load
129 that a bone can sustain prior to breaking (maximum load), and the amount of energy the bone can
130 absorb before failure (toughness). Calculations of bone mechanical properties included Young's
131 modulus, a measure of the resistance of a material to elastic deformation under load, and ultimate
132 stress, which is the maximum load normalized by the geometry of the bone midshaft.

133 *Bone histomorphometry*

134 Tibia were fixed in 10% neutral-buffered formalin for 24 hours, dehydrated, and embedded
135 in methyl metacrylate at low temperature to preserve enzymatic activity (33). Unstained 8- μ m-thick
136 sections were used for fluorescence microscopy to assess mineral apposition rate (MAR;
137 micrometers per day). Mineralizing surfaces were expressed as alizarin red-labeled surfaces per
138 bone surfaces (MS/BS; percentage), and the bone formation rate was calculated as MS/BS \times MAR
139 [bone formation rate per bone surface (BFR/BS); cubic micrometers per square micrometer per day]]
140 (34). Alternatively, sections were stained for tartrate-resistant acid phosphatase (TRAP) (Leucognost
141 SP; Merck) and counterstained with Weigert hematoxylin solution. Histomorphometric parameters
142 were measured on the trabecular bone of the metaphysis on a region of interest consisting of 2 mm
143 width below the growth plate after Goldner's trichrome staining of sections. Measurements were
144 performed using image analysis software (Tablet¹ measure; Explora Nova). Histomorphometric
145 parameters were reported in accordance with the American Society for Bone and Mineral Research
146 Committee nomenclature (35). L4 vertebrae preserved at 4° after micro-CT analysis were processed
147 in methyl metacrylate as described above and used to assess mineral and apposition rates. TRAP
148 staining was not possible in those vertebrae due to the loss of enzymatic activity.

149 *PTH measurement*

150 Serum PTH levels were measured using a commercial mouse PTH 1–84 ELISA kit (Immutopics).

151 *Statistical analysis*

152 The results were presented as mean \pm SD. Comparisons between groups for all data were
153 performed using an unpaired t test (two tailed). Differences were considered significant at $P < .05$.
154 All statistical analyses were performed using GraphPad Prism Software (GraphPad Software Inc).
155 Linear regression analysis with adjustment for body weight was performed using SPSS.

156

157 **Results**

158 *bGH mice have increased body weight and bone length compared with their littermate controls*

159 Five-month-old hemizygous male bGH mice were compared with age- and sex-matched NT
160 controls (n = 16/group). As expected, bGH transgenic mice displayed significant increases in body
161 weight (Figure 1A). Bone lengths of tibia, femora, and lumbar vertebra (total length of L4 and L5)
162 were measured using micro-CT. All bones were consistently longer in bGH mice compared with NT
163 mice (Figure 1, B–D).

164 *bGH mice have lower trabecular bone volume fraction in the tibial metaphysis compared with their*
165 *littermate controls*

166 Using micro-CT imaging, we found that the trabecular bone volume fraction (BV/TV) was
167 significantly reduced in the bGH mice compared with the NT mice, indicating that bGH mice have
168 low bone mass. This was the case when results were expressed both as direct measurements or
169 when they were adjusted for bone length differences between NT and bGH mice (Table 1). The bone
170 structural analysis showed that the lower BV/TV was due to a reduction in both trabecular thickness
171 and number, although the reduction in trabecular thickness was more highly significant (Table 1).
172 The significant decrease in BV/TV in bGH mice was confirmed by histomorphometry measurements
173 (Table 2). The significant increases in trabecular pattern factor and SMI in bGH mice indicate less
174 intertrabecular connectivity, suggesting deterioration of trabecular bone microarchitecture in those
175 mice (Table 1). The degree of anisotropy was significantly decreased in bGH mice compared with NT
176 mice (Table 1), indicating increased isotropic structure in bGH mice.

177 *bGH mice have increased bone perimeter but lower cortical bone thickness in tibiae compared with*
178 *their littermate controls*

179 Cortical bone architecture was also analyzed at 37% and 50% of tibia length from its
180 proximal end. Similar data were obtained at both lengths, and Table 1 illustrates the results at 37%
181 of tibia length. Although cortical bone area was similar in bGH and NT mice, total cross-sectional
182 area, cortical bone perimeter, and medullary area were increased and cross-sectional thickness
183 significantly decreased in bGH mice compared with NT mice (Table 1), suggesting that bone size and
184 geometry are different in bGH mice. All these differences remained highly significant after correction
185 for tibiae length. In contrast, only the decrease in cortical thickness in bGH mice remained significant
186 after adjustment for body weight.

187 *bGH mice have decreased bone cortical mineral density and changes in trabecular and cortical*
188 *structural parameters in vertebrae compared with their littermate controls*

189 BMD was evaluated in fourth and fifth lumbar vertebrae (L4 and L5). Similar results were
190 obtained for both vertebrae, and we have illustrated the results obtained on the fifth lumbar
191 vertebrae. We did not measure significant differences in the BMD of the trabecular compartment in
192 the vertebrae between bGH and NT mice (Figure 2A), whereas the BMD in the cortical compartment
193 was significantly decreased in bGH vertebrae compared with NT ones (Figure 2B). BV/TV was not
194 different in bGH and NT mice vertebrae, except when adjusted for bone length (Table 3). Trabecular
195 thickness was significantly decreased in bGH vertebrae compared with the NT group, even after

196 adjustment for length and body weight, although histomorphometry data showed only a trend for a
197 decrease (Tables 3 and 4). Other trabecular parameters were not consistently affected.
198 Significant differences were also observed in cortical bone because L4 and L5 vertebrae in bGH
199 group showed increased bone cortical area but decreased cortical thickness (Table 3). However, only
200 cortical thickness remained significant after correction for both body weight and vertebrae length.

201 *bGH mice have decreased mechanical strength in tibiae compared with their littermate controls*

202 To investigate bone mechanical properties of bGH mice, their femurs were removed at 5
203 months and subjected to three-point bending tests. Data on the mechanical strength of the femurs
204 are shown in Figure 3. Compared with the NT group, bGH had weaker bones, as illustrated by
205 significantly reduced ultimate stress (Figure 3A) and Young's modulus (Figure 3B). There was also a
206 trend for a reduced stiffness in bGH mice compared with NT mice, close to significance (Figure 3C).

207 *bGH mice have increased bone remodeling compared with their littermate controls*

208 To determine the cause of the low trabecular bone mass in bGH mice, we examined bone
209 cellular activities in the tibia of those mice, using bone histomorphometry. Histomorphometric
210 assessment confirmed our micro-CT findings that trabecular BV/TV in tibial metaphysis is
211 significantly decreased in bGH compared with NT mice (Figure 4A and Table 2). Analysis of
212 mineralizing apposition and bone formation rates using double-fluorescence labeling showed that
213 bGH mice have a higher bone formation rate than NT mice (Figure 4C). MAR was significantly
214 increased (Table 2). The percentage of TRAP-positive surfaces (representing resorption surfaces) was
215 also significantly higher in the bGH mice compared with NT mice (Figure 4B). These results indicate
216 that the bGH mice have a higher trabecular bone turnover compared with their littermate controls,
217 which is associated with a low trabecular bone mass phenotype. The increased bone formation rate
218 in bGH mice compared with their littermate controls was also observed in vertebrae (Table 4). We
219 also measured serum PTH levels in our mice, and we found significantly increased PTH levels in 5-
220 month-old male bGH mice compared with littermate controls (Figure 4D).

221

222 **Discussion**

223 This study shows that bGH mice with elevated serum GH levels have compromised bone
224 architecture, characteristic that often mimics the skeletal changes experienced by acromegaly
225 patients. The use of bGH mice is a valuable model for the study of skeletal changes in response to
226 excess GH that occur in acromegaly patients. The advantage of this experimental mouse model is
227 that there is no associated hypogonadism (36), so it is easier to decipher the skeletal effects of

228 excess GH than in acromegaly patients. There is, however, a major difference between the bGH
229 mouse model and acromegaly patients as in patients' overexpression of GH usually occurs after
230 epiphyseal closure. Conversely, overexpression of GH in bGH mice occurs in utero and through adult
231 life. Thus, it is possible that the temporal control of GH overexpression has implications on bone
232 regulation.

233 Our works shows that bGH mice have significant increases in total body weight and in bone
234 lengths. This supports previous studies that demonstrated that human GH and bGH transgenic mice
235 are larger and exhibit disproportionate skeletal gigantism (28,–30, 37, 38). Bone sizes are increased
236 in bGH mice (30), and treatment of growing rats with human GH rats leads to an increase in bone
237 size (39). Elevated levels of GH appear to be the main cause for gigantism in those mice rather than
238 an increase in mechanical loading as a result of increased body weight (40).

239 Bone architecture in bGH mice has been poorly studied. GH has complex effects on bone
240 that vary, depending on the skeletal compartments and different sites. Using high-resolution micro-
241 CT, we found that bGH mice have altered cortical and trabecular bone architecture in long bones.
242 Analysis of trabecular bone in tibia shows that despite an increase in bone length, bGH mice have
243 significantly lower bone volume fraction (BV/TV) and trabecular number and thickness than
244 littermate controls, indicating a low trabecular bone mass in those mice. In addition, measurements
245 of parameters reflecting the structure and the geometry of trabecular bone clearly demonstrate less
246 intertrabecular connectivity and more rod-like structures in trabecular bone of bGH mice,
247 representing a deterioration of trabecular bone quality that is similar to what is observed with aging
248 and in osteoporosis (41) and in agreement with most clinical studies (20). Cortical bone thickness
249 was also significantly decreased in tibia despite increases in total cross-sectional area, cortical tissue
250 perimeter, and medullary area, reflecting the bigger tibia in bGH mice. Previous micro-CT analysis of
251 GH transgenic mice did not show any major change in trabecular bone volume fraction in male mice.
252 In contrast, female transgenic mice showed an increase in trabecular bone fraction volume in
253 femora (29). This discrepancy could be due to a different mouse genetic background and/or the age
254 of the mice because the transgenic mice used in our study are older (5 mo vs 3 mo in the previous
255 study). Our resolution for micro-CT analysis of bone architecture was also 10 times higher than that
256 used in the former study (29).

257 Because there is an increased prevalence of vertebral fractures in acromegaly patients (12),
258 we also examined bone architecture and BMD in vertebrae of bGH mice. Surprisingly, there were no
259 significant changes in trabecular BMD and bone volume fraction in L4 and L5 vertebrae of bGH mice
260 compared with controls but a decrease in trabecular thickness. Cortical bone was more significantly

261 affected because bGH mice have significantly lower cortical BMD and cortical thickness in the lumbar
262 vertebrae than their controls. Although cortical bone density was also previously shown to be
263 significantly lower in femora of bGH transgenic mice (30), these results in mouse models conflict
264 with clinical records whereby elevated GH levels are often linked to increased cortical BMD in
265 humans (1, 19, 20, 42). Clinical data are, however, mostly based on BMD measurements by dual-
266 energy X-ray absorptiometry, which cannot discriminate between cortical and trabecular
267 compartments, in contrast to micro-CT or peripheral quantitative computed tomography (pQCT).
268 The view of increased cortical BMD in patients with active acromegaly is supported by the fact that
269 these patients have an increase in BMD at the forearm and/or femoral neck, two sites at which
270 cortical bone is the main determinant of bone strength, whereas BMD is less affected at the lumbar
271 spine, a site at which trabecular bone is dominant (19, 43, 44). This was corroborated in a clinical
272 study using high-resolution pQCT, which showed higher cortical density in the distal tibia in patients
273 with active acromegaly compared with controlled acromegaly (20), suggesting that high resolution
274 pQCT should allow better in vivo assessments of the bone architecture in acromegaly patients in the
275 future.

276 Interestingly, studies conducted in childhood- and adult-onset GHD have also shown
277 reduced cortical bone (45) and GH therapy in GHD patients seems to have a greater effect on cortical
278 than on trabecular bone (46). Our data support previous conclusions demonstrating that the skeletal
279 effects of GH depend on the compartment and the site analyzed, and this may be due to changes in
280 vascular supply, response to sex steroids, and/or mechanical loading (19). We used only males in our
281 study to restrict the differences in cortical density between sexes. We analyzed bone architecture at
282 two sites with a very different ratio in cortical and trabecular bone but that are also subject to
283 different loading environments. We therefore cannot exclude that the differences in bone
284 architecture between bGH mice tibiae and vertebrae depend on mechanical sensitivity to loading,
285 which is essential for the maintenance of the skeleton in both humans and animals. Previous studies
286 have shown that the GH/IGF-1 signaling pathway is regulated by in vivo mechanical loading (47).

287 At all sites examined, our data suggest a deterioration of bone architecture. This was
288 confirmed by the decreased intrinsic material properties of femora of bGH mice, leading to a
289 reduction in bone strength, which may explain the higher rate of fractures in acromegaly patients.
290 Decreased trabecular bone biomechanical competence was also observed in acromegaly patients
291 (48). Interestingly, it was shown that local production of human GH in osteoblasts in a model of
292 transgenic mice induces bone growth as expected but impaired the bones mechanical properties
293 (49). In contrast, erythroid-specific expression of human GH leads to bones with high bone density
294 and increased biomechanical properties (50). This suggests that localized GH expression could have

295 opposing effect to global GH expression as observed in our study. In models of GHD, bone
296 mechanical properties are also not always rescued with GH treatment (51). It is, however, puzzling
297 that acromegalic patients have a higher prevalence of vertebral fractures because our data suggest
298 that trabecular architecture in bGH vertebrae is less deteriorated than in tibiae.

299 The cortex also contributes to a significant part of vertebral bone strength (52) and other
300 bone quality parameters, such as collagen content, and morphology may play a role. It is also
301 important to point out that the spine in the mouse is not a good model of the spine in humans
302 because it has almost no load bearing. Bone strength depends on bone morphology and composition
303 that can be associated with changes in bone turnover rate. Our results indicate that bone turnover is
304 largely increased in the trabecular bone of adult bGH mice tibia. We also found an increase in the
305 number of mineralizing surfaces and osteoclasts on bone surfaces, suggesting that bone cell
306 numbers and activities are both stimulated in bGH mice compared with controls. To our knowledge,
307 this is the first demonstration of accelerated bone turnover in favor of bone resorption in the
308 skeleton of bGH mice, and this may explain the deterioration of bone mechanical strength in these
309 mice. Bone turnover markers in acromegaly patients are also increased (19) and GH treatment is
310 effective in enhancing bone turnover (46, 53, 54). The increased bone turnover in bGH mice suggests
311 that the deterioration of bone architecture observed in those mice is not the consequence of
312 changes occurring during bone development that can affect bone architecture later in life. The
313 increase in cortical perimeter together with the decrease in cortical thickness observed in bGH mice
314 suggest that endosteal bone resorption and periosteal bone formation are both enhanced, which
315 explains the increase in bone size. Interestingly, we found a similar increased bone formation rate in
316 the vertebral trabecular bone of bGH mice compared with controls, suggesting that bone cellular
317 activities are also stimulated in vertebrae, although this needs to be confirmed in case of osteoclast
318 activity.

319 The mechanisms leading to the enhanced bone turnover in bGH mice whose net balance is
320 bone resorption is yet unclear. Our data show increased PTH levels in bGH mice, which could
321 contribute to this greater bone turnover (55). GH transgenic mice have also hyperinsulinemia
322 despite euglycemia (56). Other possible mechanisms include stimulation by GH and IGF-1 of
323 proinflammatory cytokines that may promote osteoclastogenesis (57). A very exciting future aspect
324 of this work will be to determine which direct or indirect signaling pathways link the excess GH in
325 our mouse model to these deleterious effects on bone. GHR affects many signaling pathways, the
326 major one being the JAK/STAT but additional independent pathways have been identified (58).
327 Among the pathways affected by GHR activation and JAK2 are the MAPK and phosphatidylinositol 3-
328 kinase/Akt pathways, which play crucial roles in the differentiation, function, and survival of bone

329 cells (59). GH also regulates IGF-1 expression that has direct effects on bone via IGF-1 receptor and
330 downstream signaling cascades critical for bone cell survival and metabolism (60). It is also possible
331 that in our mouse model, the high GH tone may lead to feedback inhibition. Recent studies have
332 indicated that GHR activation induces suppression of cytokine signaling (SOCS) proteins, which in
333 turn inhibit GH signaling through a negative feedback mechanism. SOCS play important roles in
334 skeletal development and osteoclastogenesis (61).

335 In conclusion, our data collectively indicate that elevated serum GH levels have negative
336 effects on bone architecture and quality in male mice. Combining, for the first time, high-resolution
337 micro-CT measurements of skeletal architecture in trabecular and cortical compartments, bone
338 mechanical testing, and quantification of bone cellular activities, we show that bGH mice display
339 characteristics of the skeletal changes observed in acromegaly patients, which vary according to the
340 skeletal site. Our study is limited by the fact that we have only analyzed males and only at one
341 particular time point; therefore, we cannot exclude that bGH female mice may behave differently
342 because the skeletal effects of GH may be influenced by sex steroids and mechanical loading. It,
343 however, supports the notion that bone strength is decreased in acromegaly patients and that this
344 may not always be reflected in the measurement of BMD. The inability of BMD to predict fracture
345 risk in acromegaly patients is also true in diabetic patients (62) and clearly demonstrates the need
346 for a better understanding of factors affecting bone quality in patients with altered GH and IGF-1
347 metabolism.

348

349 **Acknowledgments**

350 This work was supported by the Society for Endocrinology.

351 Disclosure Summary: The authors have nothing to disclose

352

353 **Abbreviations**

354 BFR/BS: bone formation rate per bone surface

355 bGH: bovine GH

356 BMD: bone mineral density

357 BV: bone volume

358 Ct.Ar: cortical bone area

359 Ct.Pm: cortical bone perimeter

360 Ct.Th: cross-sectional thickness

361 DA: degree of anisotropy

362 GHD: GH deficiency

363 GHR: GH receptor
364 JAK: Janus kinase
365 Ma.Ar: medullary area
366 MAR: mineral apposition rate
367 micro-CT: microcomputed tomography
368 MS/BS: mineralizing surfaces per bone surface
369 NT: nontransgenic
370 pQCT: peripheral quantitative computed tomography
371 SMI: structure model index
372 STAT: signal transducer and activator of transcription
373 Tb.N: trabecular number
374 Tb.Sp: trabecular separation
375 Tb.Th trabecular thickness
376 TBPf: trabecular bone pattern factor
377 TRAP: tartrate-resistant acid phosphatase
378 Tt.Ar: total cross-sectional area
379 TV: tissue volume

380

381

382 **References**

383 1. Ohlsson C, Bengtsson BA, Isaksson OG, Andreassen TT, Słotweg MC. Growth hormone
384 and bone. *Endocr Rev.* 1998;19:55–79. [PubMed: 9494780]

385 2. Ohlsson C, Nilsson A, Isaksson OG, Lindahl A. Effect of growth hormone and insulin-like
386 growth factor-I on DNA synthesis and matrix production in rat epiphyseal chondrocytes in
387 monolayer culture. *J Endocrinol.* 1992;133:291–300.[PubMed: 1613431]

388 3. Tritos NA, Biller BM. Growth hormone and bone. *Curr Opin Endocrinol Diabetes Obes.*
389 2009;16:415–422.[PubMed: 19770650]

390 4. Vijayakumar A, Novosyadlyy R, Wu Y, Yakar S, LeRoith D. Biological effects of growth
391 hormone on carbohydrate and lipid metabolism. *Growth Horm IGF Res.* 2010;20:1–
392 7. [PMCID: PMC2815161] [PubMed: 19800274]

393 5. Gent J, van Kerkhof P, Roza M, Bu G, Strous GJ. Ligand-independent growth hormone
394 receptor dimerization occurs in the endoplasmic reticulum and is required for ubiquitin
395 system-dependent endocytosis. *Proc Natl Acad Sci USA.* 2002;99:9858–9863. [PMCID:
396 PMC125043] [PubMed: 12105275]

397 6. Giustina A, Mazziotti G, Canalis E. Growth hormone, insulin-like growth factors and the
398 skeleton. *Endocr Rev.* 2008;29:535–559. [PMCID: PMC2726838] [PubMed: 18436706]

399 7. Courtland H-W, Sun H, Beth-On M, et al. Growth hormone mediates pubertal skeletal
400 development independent of hepatic IGF-1 Production. *J Bone Miner Res.* 2011;26:761–
401 768. [PMCID: PMC3179330] [PubMed: 20928887]

402 8. Melmed S. Acromegaly pathogenesis and treatment. *J Clin Invest.* 2009;119:3189–
403 3202. [PMCID: PMC2769196][PubMed: 19884662]

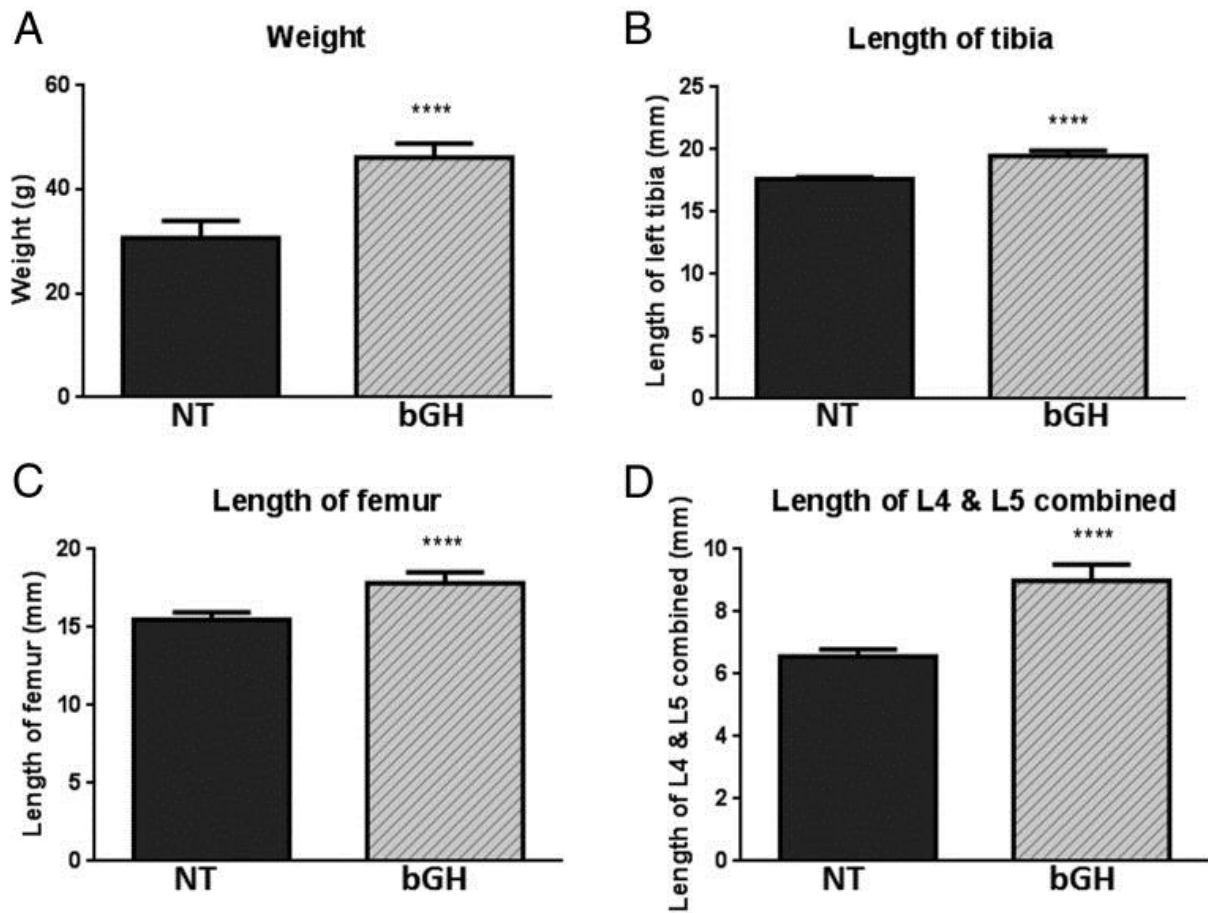
404 9. Thomas JD, Monson JP. Adult GH deficiency throughout lifetime. *Eur J Endocrinol.*
405 2009;161:S97–S106.[PubMed: 19684058]

- 406 10. Colao A, Di Somma C, Pivonello R, et al. Bone loss is correlated to the severity of growth
407 hormone deficiency in adult patients with hypopituitarism. *J Clin Endocrinol Metab.*
408 1999;84:1919–1924. [PubMed: 10372687]
- 409 11. Claessen KM, Kroon HM, Pereira AM, et al. Progression of vertebral fractures despite
410 long-term biochemical control of acromegaly: a prospective follow-up study. *J Clin*
411 *Endocrinol Metab.* 2013;98:4808–4815. [PubMed: 24081732]
- 412 12. Padova G, Borzi G, Incorvaia L, et al. Prevalence of osteoporosis and vertebral fractures
413 in acromegalic patient. *Clin Cases Miner Bone Metab.* 2011;8:37–43. [PMCID:
414 PMC3279059] [PubMed: 22461828]
- 415 13. Mazziotti G, Bianchi A, Bonadonna S, et al. Prevalence of vertebral fractures in men with
416 active acromegaly. *J Clin Endocr Metab.* 2008;93:4649–4655. [PubMed: 18827004]
- 417 14. Wassenaar MJ, Biermasz NR, Hamdy NA, et al. High prevalence of vertebral fractures
418 despite normal bone mineral density in patients with long-term controlled acromegaly. *Eur J*
419 *Endocrinol.* 2011;164:475–483. [PubMed: 21257726]
- 420 15. Mazziotti G, Bianchi A, Porcelli T, et al. Vertebral fractures in patients with acromegaly: a
421 3-year prospective study. *J Clin Endocrinol Metab.* 2013;98:3402–3410. [PubMed:
422 23771918]
- 423 16. Mormando M, Nasto LA, Bianchi A, et al. Growth hormone receptor isoforms and
424 skeletal fragility in acromegaly. *Eur J Endocrinol.* 2014;171:237–245. [PubMed: 24866575]
- 425 17. Jean Ho P, Lorraine M, Barkan A, Shaporo B. Bone mineral density of the axial skeleton in
426 acromegaly. *J Nucl Med.* 1992;33:1608–1612. [PubMed: 1517833]
- 427 18. Kayath Mj, Viera JG. Osteopenia occurs in a minority of patients with acromegaly and is
428 predominant in the spine. *Osteoporosis Int.* 1997;7:226–230.
- 429 19. Bolanowski M, Daroszewski J, Medras M, Zadrozna-Sliwka B. Bone mineral density and
430 turnover in patients with acromegaly in relation to sex, disease activity and gonadal
431 function. *J Bone Miner Metab.* 2006;24:72–78.[PubMed: 16369902]
- 432 20. Madeira M, Neto LV, de Paula Paranhos Neto F, et al. Acromegaly has a negative
433 influence on trabecular bone, but not on cortical bone, as assessed by high resolution
434 peripheral quantitative computed tomography. *J Clin Endocrinol Metab.* 2013;98:1734–
435 1741. [PubMed: 23482608]
- 436 21. Vestergaard P, Mosekilde L. Fracture risk is decreased in acromegaly: a potential
437 beneficial effect of growth hormone. *Osteoporosis Int.* 2004;15:155–159.
- 438 22. Felsenberg D, Boonen S. The bone quality framework: determinants of bone strength
439 and their interrelationships, and implications for osteoporosis management. *Clin Ther.*
440 2005;27:1–11. [PubMed: 15763602]
- 441 23. Borah B, Gross GJ, Dufresne TE, et al. Three dimensional microimaging (MRmicrol and
442 microCT), finite element modeling, and rapid prototyping provide unique insights into bone
443 architecture in osteoporosis. *Anat Rec.* 2001;265:101–110. [PubMed: 11323772]

- 444 24. Chavassieux P, Seeman E, Delmas PD. Insights into material and structural basis of bone
445 fragility from diseases associated with fractures: how determinants of the biomechanical
446 properties of bone are compromised by disease. *Endocr Rev.* 2007;28:151–164. [PubMed:
447 17200084]
- 448 25. Kopchick JJ, Bellush LL, Coschigano KT. Transgenic models of growth hormone
449 action. *Annu Rev Nutr.* 1999;19:437–461. [PubMed: 10448532]
- 450 26. Turner ND, Knapp JR, Byers FM, Kopchick JJ. Physical and mechanical characteristics of
451 tibias from transgenic mice expressing mutant bovine growth hormone genes. *Exp Biol Med.*
452 2001;226:133–139.
- 453 27. Berryman DE, List EO, Coschigano KT, Behar K, Kim JK, Kopchick JJ. Comparing adiposity
454 profiles in three mouse models with altered GH signaling. *Growth Horm IGF Res.*
455 2004;14:309–318. [PubMed: 15231300]
- 456 28. Wolf E, Rapp K, Brem G. Expression of metallothionein-human growth hormone fusion
457 genes in transgenic mice results in disproportionate skeletal gigantism. *Growth Dev Aging.*
458 1991;55:117–127. [PubMed: 1938045]
- 459 29. Eckstein F, Lochmüller EM, Koller B, et al. Body composition, bone mass and
460 microarchitectural analysis in GH-transgenic mice reveals that skeletal changes are specific
461 to bone compartment and gender. *Growth Horm IGF Res.* 2002;12:116–125. [PubMed:
462 12175649]
- 463 30. Eckstein F, Weusten A, Schmidt C, et al. Longitudinal in vivo effects of growth hormone
464 overexpression on bone in transgenic mice. *J Bone Miner Res.* 2004;19:802–810. [PubMed:
465 15068504]
- 466 31. Shah M, Kola B, Bataveljic A, et al. AMP-activated protein kinase (AMPK) activation
467 regulates in vitro bone formation and bone mass. *Bone.* 2010;147:309–319. [PMCID:
468 PMC3629687] [PubMed: 20399918]
- 469 32. Marenzana M, Greenslade K, Eddleston A, et al. Sclerostin antibody treatment enhances
470 bone strength but does not prevent growth retardation in young mice treated with
471 dexamethasone. *Arthritis Rheum.* 2011;63:2385–2395.[PubMed: 21484764]
- 472 33. Chappard D, Palle S, Alexandre C, Vico L, Riffat G. Bone embedding in pure methyl
473 methacrylate at low temperature preserves enzyme activities. *Acta Histochem.*
474 1987;81:183–190. [PubMed: 3111154]
- 475 34. Chavassieux P, Arlot M, Meunier PJ. Clinical use of bone biopsy. In: Marcus R, Feldman
476 D, Kelsey J, editors. , eds. *Osteoporosis.* 2nd ed San Diego: Academic Press; 2001:501–509.
- 477 35. Dempster DW, Compston JE, Drezner MK, et al. Standardized nomenclature, symbols
478 and units for bone histomorphometry. A 2012 update of the report of the ASBMR
479 histomorphometry nomenclature committee. *J Bone Miner Res.* 2013;28:1–16. [PMCID:
480 PMC3672237] [PubMed: 23197339]
- 481 36. Cecim M, Kerr J, Bartke A. Effects of bovine growth hormone (bGH) transgene
482 expression or bGH treatment on reproductive functions in female mice. *Biol Reprod.*
483 1995;52:1144–1148. [PubMed: 7626714]

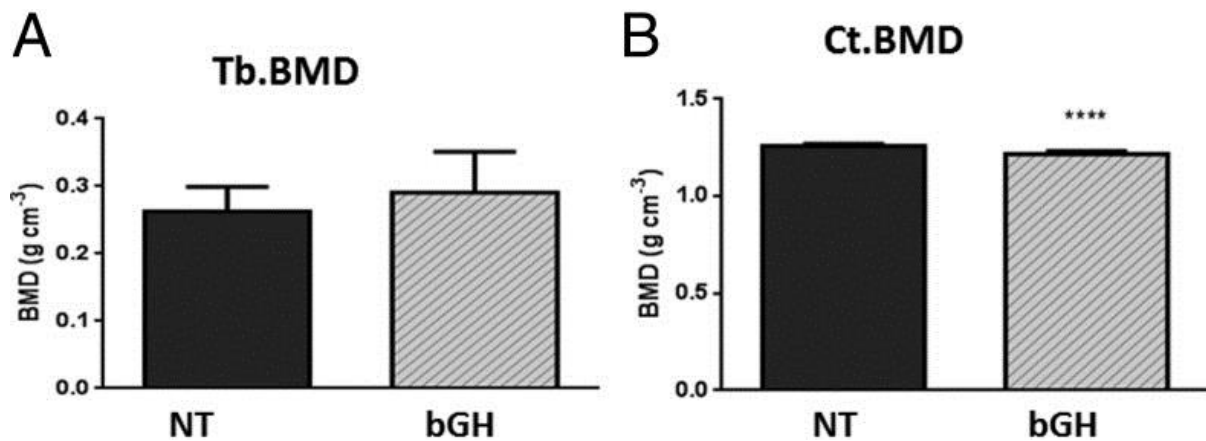
- 484 37. Wanke R, Wolf E, Hermanns W, Folger S, Buchmüller T, Brem G. The GH-transgenic
485 mouse as an experimental model for growth research: clinical and pathological
486 studies. *Horm Res.* 1992;37:74–87. [PubMed: 1427647]
- 487 38. Wolf E, Rapp K, Wanke R, et al. Growth characteristics of metallothionein-human growth
488 hormone transgenic mice as compared to mice selected for high eight-week body weight
489 and unselected controls. II. Skeleton *Growth Dev Aging.* 1991;55:237–248.
- 490 39. Rosen HN, Chen V, Citadini A, et al. Treatment with growth hormone and IGF-1 in
491 growing rats increases bone mineral content but not bone mineral density. *J Bone Miner
492 Res.* 1995;10:1352–1358. [PubMed: 7502707]
- 493 40. Palmer AJ, Chung M-Y, List EO, et al. Age-related changes in body composition of bovine
494 growth hormone transgenic mice. *Endocrinology.* 2009;150:1353–1360. [PMCID:
495 PMC2654748] [PubMed: 18948397]
- 496 41. Borah B, Dufresne TE, Chmielewski PA, Johnson TD, Chines A, Manhart MD. Risedronate
497 preserves bone architecture in postmenopausal women with osteoporosis as measured by
498 three-dimensional microcomputed tomography. *Bone.* 2004;34:736–746. [PubMed:
499 15050906]
- 500 42. Kaji H, Sugimoto T, Nakaoka D, Okimura Y, Abe H, Chihara K. Bone metabolism and body
501 composition in Japanese patients with active acromegaly. *Clin Endocrinol (Oxf).*
502 2001;55:175–181. [PubMed: 11531923]
- 503 43. Biermasz N, Hamdy NAT, Pereira AM, Romijn JA, Roelsema F. Long-term maintenance of
504 the anabolic effects of GH on the skeleton in successfully treated patients with
505 acromegaly. *Eur J Endocrinol.* 2005;152:53–60. [PubMed: 15762187]
- 506 44. Chiodini I, Trischitta V, Carnevale V, Liuzzi A, Scillitani A. Bone mineral density in
507 acromegaly: does growth hormone excess protect against osteoporosis? *J Endocrinol Invest.*
508 2001;24:288–291. [PubMed: 11383916]
- 509 45. Murray RD, Adams JE, Shalet SM. A densitometric and morphometric analysis of the
510 skeleton in adults with varying degrees of growth hormone deficiency. *J Clin Endocrinol
511 Metab.* 2006;91:432–438. [PubMed: 16278268]
- 512 46. Bravenboer N, Holzmann PJ, Ter Maaten PJ, Stururman LM, Roos JC, Lips P. Effect of
513 long-term growth hormone treatment on bone mass and bone metabolism in growth
514 hormone-deficient men. *J Bone Miner Res.* 2005;20:1778–1784.[PubMed: 16160735]
- 515 47. Rejnders CM, Bravenboer N, Holzmann PJ, Bhoelan F, Blankenstein MA, Lips P. In vivo
516 mechanical loading modulates insulin-like growth factor binding protein-2 gene expression
517 in rat osteocytes. *Calcif Tissue Int.* 2007;80:137–143. [PMCID: PMC1914289] [PubMed:
518 17308996]
- 519 48. Ueland T, Ebbesen EN, Thomsen JS, et al. Decreased trabecular bone biomechanical
520 competence, apparent density, IGF-II and IGHBP-5 content in acromegaly. *Eur J Clin Invest.*
521 2002;32:122–128. [PubMed: 11895459]
- 522 49. Tseng KF, Bonadio JF, Stewart TA, Baker AR, Goldstein SA. Local expression of human
523 growth hormone in bone results in impaired mechanical integrity in the skeletal tissue of
524 transgenic mice. *J Orthop Res.* 1996;14:598–604.[PubMed: 8764869]

- 525 50. Steinke B, Patwardhan AG, Havey RM, King D. Human growth hormone transgene
526 expression increases the biomechanical structural properties of mouse vertebrae. *Spine*.
527 1999;24:1–4. [PubMed: 9921583]
- 528 51. Kristensen E, Hallfrimsson B, Morck DW, Boyd SK. Microarchitecture, but not bone
529 mechanical properties, is rescued with growth hormone treatment in a mouse model of
530 growth hormone deficiency. *Int J Endocrinol*. 2012;2012:294965. [PMCID:
531 PMC3312192] [PubMed: 22505889]
- 532 52. Roux JP, Wegrzyn J, Arlot ME, et al. Contribution of trabecular and cortical
533 compartments to biomechanical behaviour of human vertebrae: an ex vivo study. *J Bone*
534 *Miner Res*. 2010;25:356–361. [PubMed: 19653808]
- 535 53. Gotherstrom G, Svensson J, Koranyi J, et al. A prospective study of 5 years of GH
536 replacement therapy in GH-deficient adults: sustained effects on body composition, bone
537 mass and metabolic indices. *J Clin Endocrinol Metab*. 2001;86:4657–4665. [PubMed:
538 11600522]
- 539 54. Bredella MA, Gerweck AV, Barber LA, et al. Effects of growth hormone administration for
540 6 months on bone turnover and bone marrow fat in obese premenopausal women. *Bone*.
541 2014;62:29–35. [PMCID: PMC4014200][PubMed: 24508386]
- 542 55. Kamenicky P, Blanchard A, Gauci C, et al. Pathophysiology of renal calcium handling in
543 acromegaly: what lies behind hypercalciuria? *J Clin Endocrinol Metab*. 2012;97:2124–
544 2133. [PubMed: 22496496]
- 545 56. Kopchick JJ, List EO, Kelder B, Gosney ES, Berryman DE. Evaluation of growth hormone
546 (GH) action in mice: discovery of GH receptor antagonists and clinical indications. *Mol Cell*
547 *Endocrinol*. 2014;386:34–45. [PMCID: PMC3943600] [PubMed: 24035867]
- 548 57. Locatelli V, Bianchi VE. Effect of GH/IGF-1 on bone metabolism and osteoporosis. *Int J*
549 *Endocrinol*. 2014;2014:235060. [PMCID: PMC4132406] [PubMed: 25147565]
- 550 58. Brooks AJ, Wei Wooh J, Tunny KA, Waters MJ. Growth hormone receptor; mechanism of
551 action. *Int J Biochem Cell Biol*. 2008;40:1984–1989. [PubMed: 17888716]
- 552 59. Marie PJ. Signaling pathways affecting skeletal health. *Cur. Osteoporosis Rep*.
553 2012;10(3):190–198.
- 554 60. Guntur AR, Rosen CJ. IGF-1 regulation of key signalling pathways in bone. *Bonekey Rep*.
555 2013;2:437. [PMCID: PMC3818534] [PubMed: 24422135]
- 556 61. Ahmed SF, Farquharson C. The effect of GH and IGF1 in linear grow and skeletal
557 development and their modulation by SOCS proteins. *J Endocrinol*. 2010;206:249–
558 259. [PubMed: 20631046]
- 559 62. Yamamoto M, Yamaguchi T, Yamauchi M, Kaji H, Sugimoto T. Diabetic patients have an
560 increased risk of vertebral fractures independent of BMD and diabetic complications. *J Bone*
561 *Miner Res*. 2009;24:702–709. [PubMed: 19049338]



565
566 **Figure 1: bGH mice have increased body weights and bone lengths.**

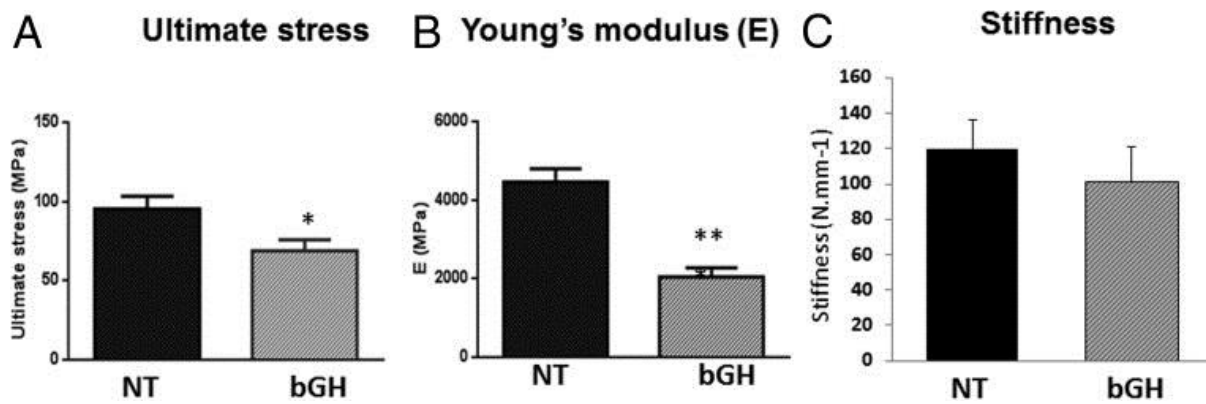
567
568 NT and bGH mice were weighed at 5 months of age and lengths of tibiae, femora, and lumbar
569 vertebrae measured using micro-CT. Body weights (A) and lengths of tibiae (B), femora (C), and
570 vertebrae (combined L4 and L5) (D) of bGH and NT mice are shown. Values are mean ± SD of n = 16
571 mice/group. ****, P < .0001 NT vs bGH mice.



572
573
574
575
576
577
578
579
580
581
582
583
584
585
586

Figure 2: bGH mice have decreased cortical BMD but not trabecular BMD in vertebrae.

Cortical and trabecular BMD were assessed by micro-CT in lumbar vertebrae L5 vertebral body from NT and bGH mice aged 5 months. L5 vertebra vertebral body trabecular BMD (A) and L5 vertebra vertebral body cortical BMD (B) in bGH and NT mice. Bars represent mean \pm SD of nine mice per group. ****, $P < .0001$ NT vs bGH mice. Tb.BMD, trabecular BMD; Ct.BMD, cortical BMD.



587
588
589
590
591
592
593
594
595
596
597

Figure 3: Mechanical testing (three point bending) of femora from bGH and NT mice.

Biomechanical properties of the excised mouse femurs in NT and bGH mice aged 5 months using the three-point bending test, which tested for ultimate stress (A), Young's modulus (B), and stiffness (C). Bars represent mean \pm SD of six mice per group. *, $P < .05$, **, $P < .001$ NT vs bGH mice.

598 **Table 1:** Trabecular and Cortical Bone Parameters in Tibiae of NT and bGH Mice Aged 5 Months

	NT Mice	bGH Mice	Results Expressed as a Ratio of Tibia Length (×100)	
			NT Mice	bGH Mice
BV/TV, %	5.430 ± 0.647	3.061 ± 0.408 ^a	30.802 ± 10.304	15.685 ± 6.667 ^b
Tb.N, 1/mm	1.640 ± 0.245	1.114 ± 0.155 ^c	9.304 ± 3.980	5.706 ± 2.382 ^c
Tb.Th, mm	0.035 ± 0.002	0.028 ± 0.001 ^b	0.201 ± 0.035	0.144 ± 0.015 ^b
Tb.Sp, mm	0.373 ± 0.038	0.391 ± 0.039	2.115 ± 0.815	2.016 ± 0.760
TBPf, 1/mm	8.873 ± 4.373	31.13 ± 3.835 ^b	50.220 ± 70.117	160.118 ± 66.80 ^b
SMI	1.208 ± 0.133	1.785 ± 0.105 ^a	6.844 ± 2.521	9.189 ± 1.815 ^a
DA	2.117 ± 0.062	1.793 ± 0.063 ^a	12.006 ± 1.103	9.211 ± 1.034 ^d
Tt.Ar, mm ²	1.343 ± 0.036	1.826 ± 0.101 ^b	7.608 ± 0.527	9.434 ± 1.149 ^a (N)
Ct.Ar, mm ²	0.781 ± 0.021	0.793 ± 0.031	4.427 ± 0.296	4.107 ± 0.386
Ct.Pm, mm	11.87 ± 0.315	16.15 ± 0.743 ^d	67.266 ± 5.165	83.528 ± 8.470 ^a (N)
Ct.Th, mm	0.131 ± 0.002	0.098 ± 0.002 ^d	0.746 ± 0.023	0.512 ± 0.043 ^d
Ma.Ar, mm ²	0.561 ± 0.017	1.032 ± 0.074 ^d	3.180 ± 0.241	5.326 ± 0.861 ^d (N)

599

600 Abbreviation: N, nonsignificant after adjustment by body weight.

601 Results are mean ± SD 16 mice/group.

602 ^aP < .01, vs NT mice.

603 ^bP < .001, vs NT mice.

604 ^cP < .05, vs NT mice.

605 ^dP < .0001 vs NT mice.

606

607

608

609

610

611

612

613

614 **Table 2:** Static and Dynamic Trabecular Bone Parameters in bGH Mice Tibiae Compared With NT
 615 Tibiae

Histomorphometry Parameters	NT	bGH
BV/TV, %	14.225 ± 1.549	8.490 ± 2.867 ^a
Tb.N, 1/mm	3.440 ± 0.582	2.380 ± 0.673
Tb.Th, mm	0.042 ± 0.009	0.035 ± 0.003
Tb.Sp, mm	0.255 ± 0.042	0.412 ± 0.150 ^a
MS/BS, %	24.34 ± 6.49	40.54 ± 8.34 ^a
MAR, μm/d	1.546 ± 0.413	2.329 ± 0.290 ^a
BFR/BS, μm ³ /μm ² /d	0.387 ± 0.189	1.001 ± 0.163 ^a
Oc.S/BS, μm	6.623 ± 1.038	9.895 ± 0.306 ^a
Oc.N/BS, 1/mm	2.19 ± 0.54	2.82 ± 0.46

616

617 Mean ± SD (five and six mice per group).

618 ^aP < .05 vs NT.

619 **Table 3:** Trabecular and Cortical Bone Parameters in Vertebrae of NT and bGH Mice Aged 5 Months
 620

	NT Mice	bGH Mice	Results Expressed as a Ratio of Vertebrae Length	
			NT mice	bGH Mice
BV/TV, %	5.699 ± 1.120	6.151 ± 1.294	1.718 ± 0.323	1.409 ± 0.286 ^a
Tb.N, 1/mm	1.578 ± 0.173	2.077 ± 0.357 ^b	0.476 ± 0.049	0.475 ± 0.072
Tb.Th, mm	0.035 ± 0.004	0.029 ± 0.001 ^b	0.011 ± 0.001	0.006 ± 0.001 ^b
Tb.Sp, mm	0.418 ± 0.026	0.462 ± 0.055 ^a	0.126 ± 0.009	0.105 ± 0.010 ^b
TBPF, 1/mm	-1.515 ± 4.94	-6.590 ± 6.951	-0.446 ± 1.512	-1.454 ± 1.544
SMI	0.739 ± 0.274	0.697 ± 0.235	0.224 ± 0.087	0.161 ± 0.058
DA	1.898 ± 0.544	1.604 ± 0.233 ^a	0.572 ± 0.154	0.368 ± 0.054 ^b
Tt.Ar, mm ²	0.428 ± 0.017	0.478 ± 0.177	0.129 ± 0.035	0.109 ± 0039
Cs.Ar, mm ²	0.278 ± 0.027	0.326 ± 0.061 ^b	0.084 ± 0.007	0.074 ± 0.010 ^a (N)
Cs.Pm, mm	12.23 ± 0.632	17.60 ± 2.576 ^c	3.698 ± 0.210	4.017 ± 0.357
Cs.Th, mm	0.045 ± 0.003	0.036 ± 0.003 ^c	0.013 ± 0.001	0.008 ± 0.001 ^c
Ma.Ar, mm ²	0.149 ± 0.100	1.152 ± 0.090	0.045 ± 0.030	0.034 ± 0.031

621

622 Abbreviation: N, nonsignificant after adjustment by body weight.

623 ^aP < .05 vs NT mice.

624 ^bP < .01 vs NT mice.

625 ^cP < .0001 vs NT mice.

626

627

628

629 **Table 4:** Static and Dynamic Trabecular Bone Parameters in bGH Mice Vertebrae Compared With NT
 630 Vertebrae

631

Histomorphometry Parameters	NT	bGH
BV/TV, %	16.532 ± 3.291	15.198 ± 2.766
Tb.N, 1/mm	4.571 ± 0.451	4.754 ± 0.837
Tb.Th, mm	0.036 ± 0.004	0.032 ± 0.004
Tb.Sp, mm	0.184 ± 0.025	0.185 ± 0.043
MS/BS, %	38.70 ± 2.869	55.60 ± 4.375 ^a
MAR, μm/d	2.081 ± 0.155	3.139 ± 0.175 ^a
BFR/BS, μm ³ /μm ² /d	0.808 ± 0.116	1.719 ± 0.191 ^a

632

633 Mean ± SD (seven to nine mice per group).

634 ^aP < .01 vs NT.